HNPS Advances in Nuclear Physics

Hellenic Nuclear Physics Society

HNPS Advances in Nuclear Physics

Proceedings of the
13th Symposium
of the Hellenic Nuclear
Physics Society

University of Ioannina
30 and 31 May 2003

Editors
N.G. Nicolis
T.S. Kosmas

The ^{135}Cs(n,γ) cross section at 30 and 500 keV

N. Patronis, P. A. Assimakopoulos, S. Dababneh, M. Heil, F. Kaeppeler, D. Karamanis, P. E. Koehler, R. Plag

The ^{135}Cs(n,γ) cross section at 30 and 500 keV

N. Patronis [a] , P.A. Assimakopoulos [a], S. Dababneh [b,1] M. Heil [b],
F. Käppeler [b], D. Karamanis [a] P. E. Koehler [c] R. Plag [b]

[a]*Nuclear Physics Laboratory, Department of Physics, The University of Ioannina,
45110 Ioannina, Greece*

[b]*Forschungszentrum Karlsruhe, Institut für Kernphysik, 76021 Karlsruhe,
Germany*

[c]*Physics Division, Oak Ridge National Laboratory, Oak Ridge, TN 37831, USA*

Abstract

The neutron capture cross section of the unstable isotope ^{135}Cs was measured relative to that of gold by means of the activation method. The sample was produced by ion implantation in a high resolution mass separator and irradiated with quasi-monoenergetic neutrons at 30 keV and 500 keV, using the ^{7}Li(p,n)^{7}Be reaction. After the irradiations at the above energies, one more irradiation with thermal neutrons was used for defining the sample mass and for measuring the half-life of ^{136}Cs. The neutron capture cross section was determined as 164 ± 10 mbarn and 34.8 ± 3.0 mbarn at 30 keV and 500 keV, respectively, and were used to normalize the theoretically derived cross section shape.

1 Introduction

The neutron capture cross section of ^{135}Cs in the keV region is required for two reasons. It determines the amount of radioactive cesium in burnt fuel elements of fast reactors and it contributes to a quantitative interpretation of the isotopic Ba abundances in terms of the temperature during stellar He burning.

Nucleosynthesis by the slow neutron capture process (*s* process) is characterized by neutron capture times, which are typically much longer than the

---

Email address: me00470@cc.uoi.gr (N. Patronis).
[1] On leave from: Faculty of Applied Sciences, Al-Balqa Applied University, Salt 19117, Jordan.

half-lives against β-decay [1]. Consequently, the reaction path in the N,Z plane follows the valley of stability as sketched in Fig. 1. However, some unstable nuclei are sufficiently long-lived that neutron capture can compete with β-decay. These nuclei act as branching points in the reaction path of the s process. Several such branchings are indicated in the example of Fig. 1. The most prominent of these branchings occurs at ^{134}Cs, whereas all others are comparably weak and have minor impact on the final Ba abundances. Apart from its strength, the main importance of the ^{134}Cs branching lies in the fact that it determines the abundance ratio of ^{134}Ba and ^{136}Ba. Both isotopes are of pure s-process origin since they are shielded from possible r-process contributions by their stable Xe isobars. Accordingly, from the reliable quantitative description of the branching valuable information with regard to the physical conditions during the s process can be obtained. In the present case, this refers to the proper combination of neutron density and temperature. The sensitivity to temperature results from the fact that the first excited state of ^{134}Cs starts to be populated by the hot stellar photon bath at temperatures in excess of 10^8 K. Allowed β-decay from that state results in a strong reduction of the half-life [2].

Since the specific activity of ^{134}Cs is prohibitive for direct measurements, improvement of the capture rate can be achieved by normalizing statistical model calculations at experimental cross sections for the neighboring isotopes. Accurate experimental data for the only stable isotope, ^{133}Cs, were complemented by a first measurement on ^{135}Cs by Jaag et al. [3] in a quasi-stellar neutron spectrum at the stellar thermal energy $kT \simeq 25 \; keV$. However, recent stellar s-process models require neutron capture rates over a wider temperature range from $kT \simeq 8$ keV to $kT \simeq 26$ keV [1,4]. Therefore, in this work the neutron capture cross section was measured at two distinct neutron energies of 30 keV and 500 keV in order to normalize the theoretically calculated cross section, which then can be used to obtain the required rates as a function of temperature.

An additional motivation arises from the fact that ^{135}Cs is an important fission product. Due to its large fission yield and its long half-life it contributes significantly to the long-term hazards of nuclear waste. The exact amount of ^{135}Cs at the end of the fuel cycle depends strongly on its neutron capture cross section, which governs its transmutation rate during burn-up. For thermal reactors, the (n_{th}, γ) cross section has been measured with good accuracy [5–7], but for fast reactors, e.g. for the currently investigated ADS systems [8], this cross section has to be known for neutron energies up to 1 MeV.
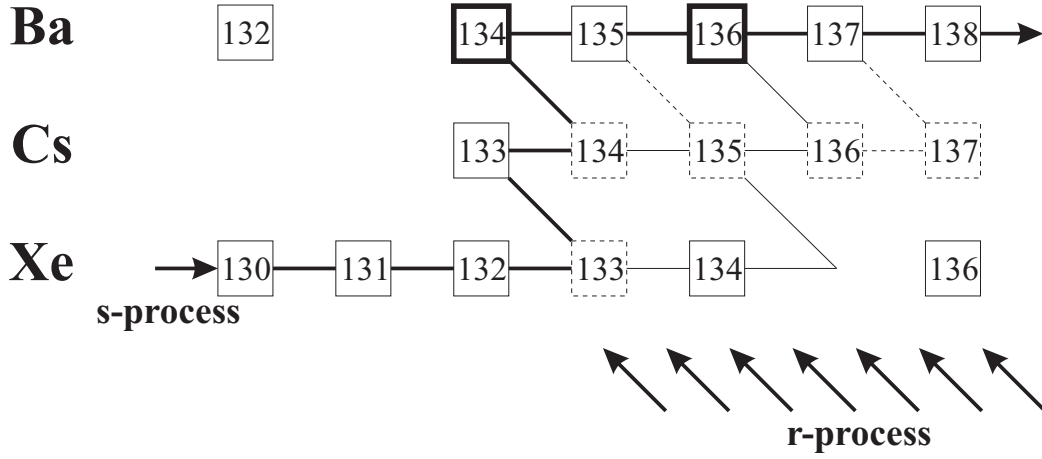
Fig. 1. The *s*-process path in the Xe-Cs-Ba region, which includes the important branching point ^{134}Cs. This branching determines the isotopic ratio of the *s*-only isotopes ^{134}Ba and ^{136}Ba, which are shielded against abundance contributions from the *r*-process region (indicated by arrows) by their stable Xe isobars. Note that ^{135}Cs is practically stable on the time scale of the *s* process, but decays afterwards and contributes to the final ^{135}Ba abundance.

2 Measurements

2.1 Experimental method

The neutron capture cross section on ^{135}Cs was measured relative to that of gold, using the activation technique. This technique offers the high sensitivity, which is essential since measurements on radioactive isotopes have to be carried out with very small samples in order to keep the background from radioactive decay at a manageable level. In total, four irradiations were carried out, the first three at the Karlsruhe 3.7 MV Van de Graaff accelerator and the fourth at the TRIGA reactor of the University of Mainz. The irradiations at the Van de Graaff were separated by waiting times of three months, corresponding to seven half-lives of the induced ^{136}Cs activity. In order to obtain comparable statistics, the measurement was carried out by one activation at 30 keV and two at 500 keV. Each irradiation lasted for about two weeks and was followed by two weeks of measurement of the induced activity. During the irradiation the gold foils were replaced approximately every three days because of the 2.7 d half-life of ^{198}Au to avoid saturation effects in the determination of integrated neutron flux. Variations in the neutron flux were continuously monitored by a ^{6}Li-glass detector.

The last irradiation was carried out with reactor neutrons in order to define the number of ^{135}Cs nuclei in the sample via the well-known thermal neutron capture cross section [7]. Following the reactor irradiation, the induced activity
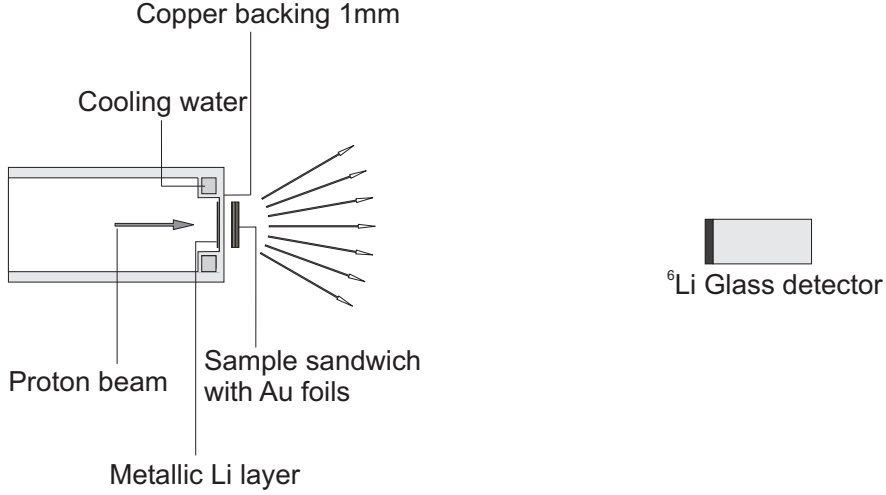
3

Fig. 2. Experimental setup during irradiation. The samples were located in the high flux close to the lithium target, and the distance between target and ^{6}Li-glass detector was 1 m.

was measured using the same detector setup as for the activations at 30 keV and 500 keV. This had the advantage that sample-related corrections, the detector efficiency, and geometry effects were canceled out.

2.2 Irradiations

At the accelerator, neutrons were produced via the ^{7}Li(p,n)^{7}Be reaction by bombarding metallic Li targets evaporated onto a 1.0 mm thick Cu backing. Proton beam currents were typically kept between 90 and 100 μA. The targets were cooled using lateral heat conduction through the copper backing to a surrounding water channel of 8 mm inner diameter (Fig. 2). The thickness of the Li targets were 30 and 10 μm for the runs at 30 and 500 keV, respectively. The Li layers were 6 mm in diameter, equal to the sample. The Cs sample was sandwiched between gold foils, also 6 mm in diameter and 0.03 mm thick. The distance of the sample sandwich to the lithium target was 1.5 mm during the 30 keV run and 8 mm during the 500 keV run.

Fig. 2 shows also the ^{6}Li-glass detector, which was located 1 m from the target at 0° with respect to the beam axis. Before the irradiations, this detector was used to select the proper proton energy by a time of flight (TOF) measurement of the neutron spectrum. For this purpose, the accelerator was operated in pulsed mode. During the irradiation the detector served to measure the neutron yield at regular time intervals. This neutron flux history was used in the analysis for off-line correction of the fraction of ^{135}Cs nuclei, which decayed already during irradiation.

4

The induced activity of the cesium sample was measured with two Clover type HPGe detectors (Eurisys). Each detectors combines four independent n-type Ge crystals in a common cryostat [9]. The Clover detectors were placed face-to-face in close geometry (Fig. 3). The distance between the Al windows of the detectors was fixed by the sample holder at 5.2 mm. The sample was positioned exactly in the mid plane of the two Clovers centered on their common axis. The individual Clover crystals were approximately 50 mm in diameter and 70 mm long.

The data acquisition system (DAQ) MPA-WIN (FAST Comptec) was used to store the detector signals event by event, thus achieving great flexibility on off-line analysis [10,14]. The corresponding output file consisted of blocks, called "events", each containing eight registers containing the energy signals of the individual crystals. If a hit was registered in one ADC, all other ADCs were read within a specified coincidence time of 4.1 μs and the whole sequence was stored as a single event. The absolute peak efficiency of this setup for the 818.5 keV line in the decay of ^{136}Cs was $\epsilon_\gamma = (1.069 \pm 0.017) \cdot 10^{-1}$ [10]. The high detection efficiency the γ spectrometer was instrumental for accumulating satisfactory statistics from the weak activities obtained with the minute ^{136}Cs sample.

The activity of the Au foils was measured with a 40 cm^3 n-type HPGe detector. The Au foils were placed 76 mm from the window of the detector. At this distance, corrections for pile-up or summing effects were negligibly small. In this case, the absolute peak efficiency for the 412 keV line from the decay of ^{198}Au was $\epsilon_\gamma = (2.20 \pm 0.03) \cdot 10^{-3}$.

The same detector was used for measuring the activity of the Re foil after the reactor irradiation. In this case, the Re foil had to be placed at 1 m distance from the detector in order to keep the counting rate sufficiently low.

2.4 *Neutron spectra*

The neutron energy distributions in the sample were calculated from the double differential cross section of the ^{7}Li(p,n)^{7}Be reaction using a C++ computer code NYIELD (developed from N. Patronis) based on Ref. [11]. The code was verified by comparison with the experimental neutron spectrum of Ratyn-ski & Käppeler [12] as shown in Fig. 4 and also via the TOF measurements performed within this experiment. In all cases the calculated spectra were consistent with the measurements.
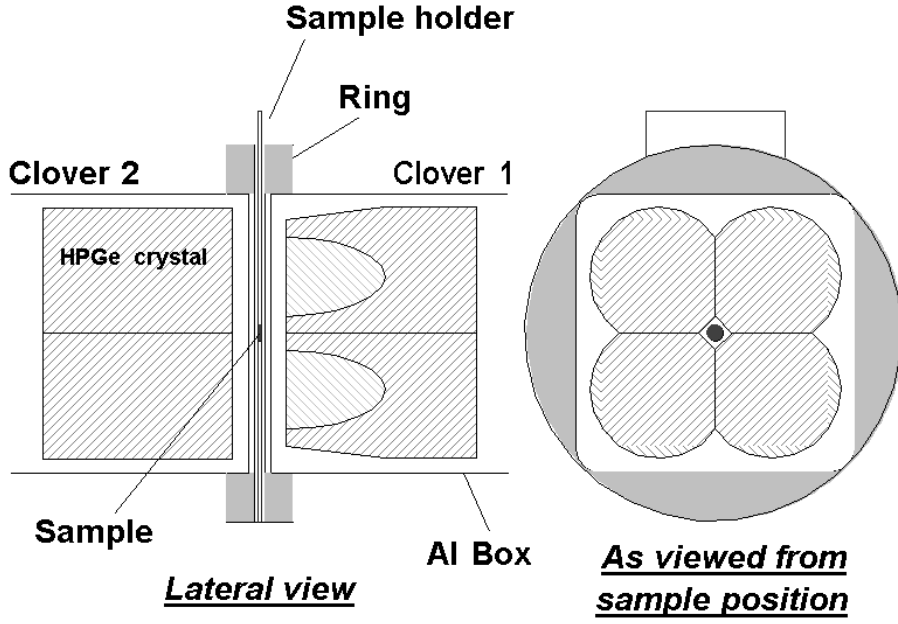
Fig. 3. Setup of the Clover detectors. The close geometry required an exact and reproducible positioning of sample and detectors, which was achieved with a special sample holder.

The spectrum at $E_n = 30$ keV was obtained by adjusting the proton beam energy to 1892 keV, 11 keV above the reaction threshold and by using a thick Li target. At this energy, the reaction kinematics restrict the emitted neutrons to a forward cone with an opening angle of $65°$. For the runs at $E_n = 500$ keV, the proton energy was 2284 keV, where neutrons are emitted in all directions. At this energy, the neutron spectrum seen by the sample was determined by means of the GEANT4 Monte Carlo (MC) code [13]. The MC technique was preferred in this case since it allows one to determine the effect of the background neutrons for the specific experimental setup, including the proper angular distribution of the source neutrons. The resulting neutron spectra for the 30 keV and 500 keV runs are presented in Fig. 5.

The neutron spectrum during the reactor irradiation is composed of the true Maxwellian spectrum at thermal energies and an epithermal component with a typical $1/E_n$ behavior, which is taken into account by the resonance integral. At the irradiation position the ratio of epithermal flux with $E_n >0.4$ eV and the thermal flux was 4/70.
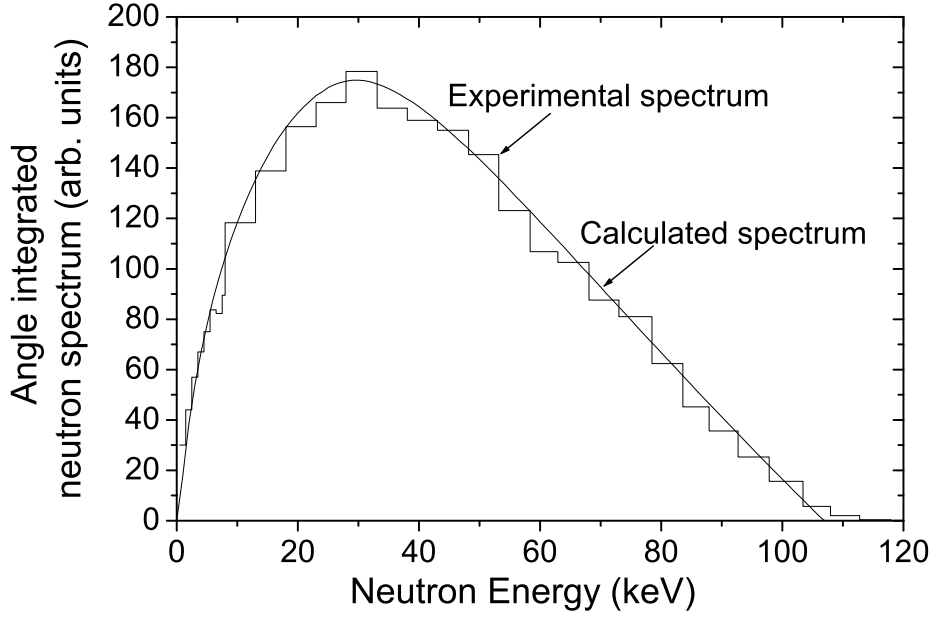
Fig. 4. The calculated neutron spectrum compared to the experimentally deduced spectrum from Ratynski & Käppeler [12].

2.5 The ^{135}Cs target

The ^{135}Cs sample used in this work was produced at Los Alamos National Laboratory with a high resolution mass separator. It was specified to contain $1.8 \cdot 10^{15}$ ^{135}Cs atoms, corresponding to a total mass of ~ 400 ng, implanted in a graphite disc 0.1 mm in thickness and 6 mm in diameter. A small remaining ^{137}Cs impurity of 167 Bq could be used to monitor the sample mass throughout the measurements. The sample disk was canned in a circular graphite box with 0.8 mm thick walls.

3   Results and discussion

3.1 Cross section

The neutron capture cross section of the unstable ^{135}Cs for the energy spectra of Fig. 5 was found equal to 164±10 and 34.8±3.0 mbarn at 30 and 500 keV respectively. For direct comparison, the cross section provided in the ENDF/B-VI library (http://www.nndc.bnl.gov/nndc/endf/endfintro.html) was folded with the experimental neutron spectra. As shown in Table 1 the experimental
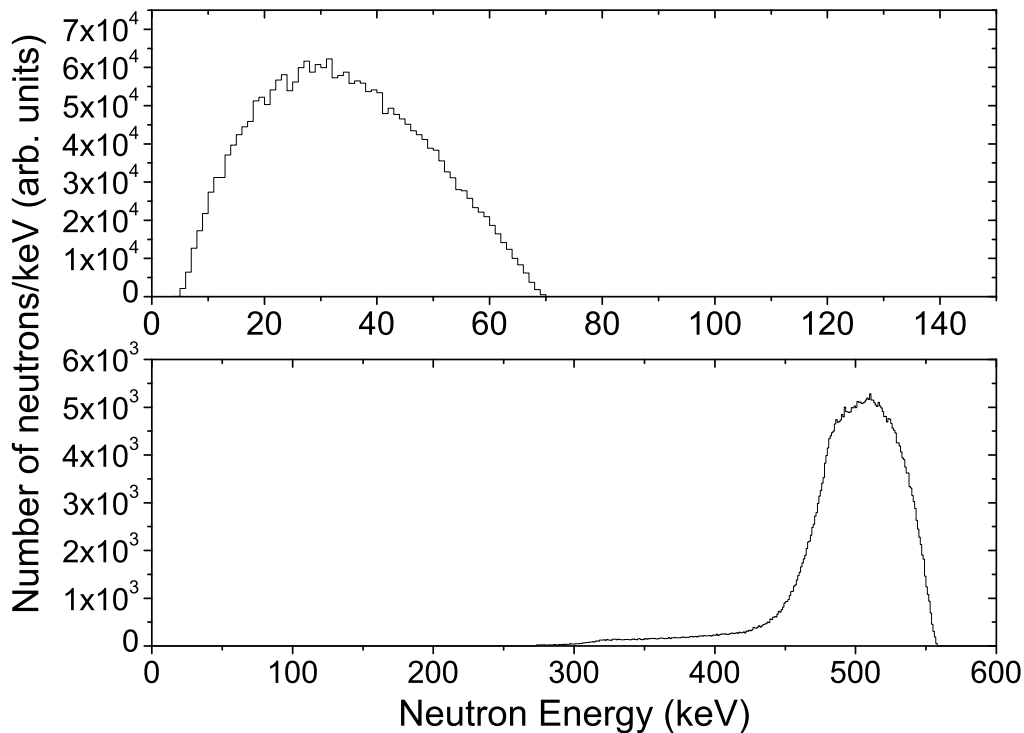
7

Fig. 5. The neutron energy spectra seen by the Cs sample in the irradiations at 30 keV (upper panel) and 500 keV (lower panel), as deduced with the NYIELD code and the GEANT4 calculations.

results are 20% lower than the calculated values of the ENDF/B-VI data base. However, this factor being equal for both energies indicates that the shape of the evaluated cross section follows the experimental points.

Based on the experimental data, refined statistical model calculations were performed to obtain the (n,γ) cross sections of all unstable Cs isotopes. The results of the theoritical calculations were used to determine the Maxwellian averaged cross section values for a set of thermal energies characteristic of the helium burning scenarios of the thermally pulsing AGB stars.The astrophysical aspects as well as a more detailed description of this work can be found elsewere [14].

3.2   Half-life of ^{136}Cs

Discrepancies in the half-life of ^{136}Cs between the values of Katoh et al. [7] (12.63 $\pm$ 0.04 d) and the most recent compilation [15] (13.16 $\pm$ 0.03 d) prompted us to resolve this problem by measuring the decay curve after the reactor activation. The intensities of the 819 and 1048 keV lines from the de-

Table 1
The measured and evaluated capture cross sections (in mbarn)

Energy (keV)	Experiment	(ENDF/B-VI)	Ratio
30 keV	164±10	204	0.804
500 keV	34.8±3.0	43.6	0.798

Table 2
Experimental half-life of ^{136}Cs

Transition energy (keV))	Half-life (d)
818.5	13.04±0.03
1048	13.04±0.04

cay of ^{136}Cs were determined daily during a period of 37 d (Fig. 6). In all these runs, a statistical uncertainty of less than 1% was achieved. The fit of the respective decay curves provided perfectly consistent results or both transitions (Table 2). The combined value of 13.04 ± 0.03 d is compatible with Ref. [15] but deviates from the measurement of Katoh et al. [7] by 10 standard deviations.

Particular attention was paid to the claim [7] that previous half-life measurements may have had problems with the pile-up corrections. At the start of this measurement, the counting of the Clover detectors was 2.3 kHz, corresponding to ~285 counts/sec for each of the eight independent Ge crystals. This rate was sufficiently low, that the pile-up correction was negligible.
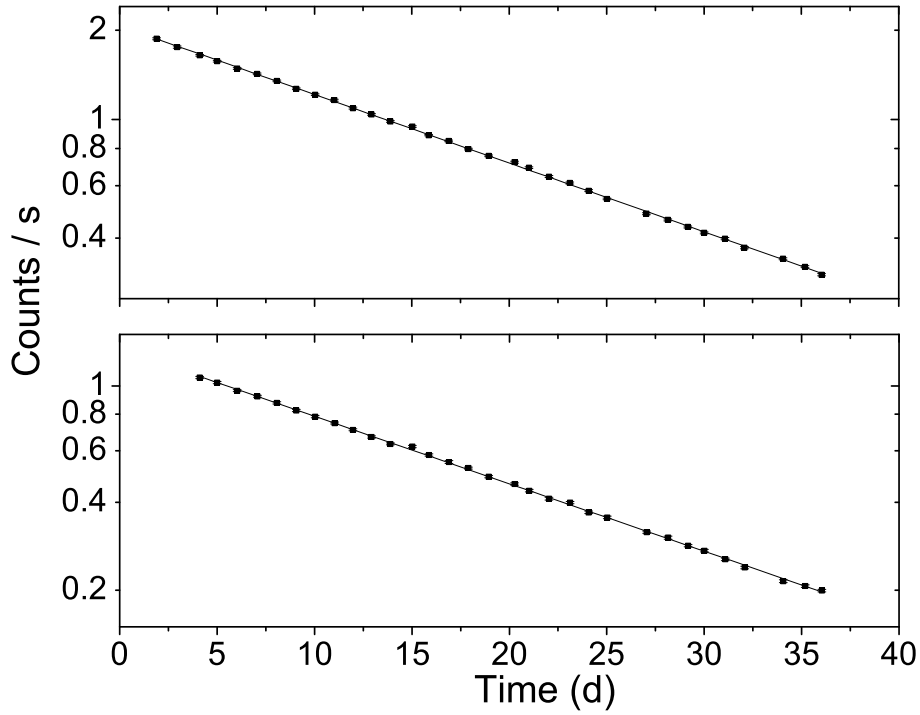
Acknowledgements

9

Fig. 6. The decay curve of ^{136}Cs obtained from the counting rates of the transitions at 819 keV and 1048 keV (upper and lower panel, respectively).

References

[1] F. Käppeler, Progr. in Part. and Nuclear Physics 43 (1999) 419

[2] K. Takahashi and K. Yokoi, Atomic Data Nucl. Data Tables 36 (1987) 375

[3] S. Jaag, F. Käppeler, P. Koehler, Nuclear Physics A621 (1997) 247c

[4] M. Busso, R. Gallino, and G. J. Wasserburg, Annu. Rev. Astron. Astrophys. 37 (1999) 239

[5] N. Sugarman, The Physical Review 75 (1949) 1473

[6] A. B. Baerg, F. Brown, and M. Lounsbury, Canadian Journal of Physics 36 (1958) 863

[7] T. Katoh, S. Nakamura, H. Harada, Y. Hatsukawa, N. Shinohara, K. Hata, K. Kobayashi, S. Motoishi, and M. Tanase, Journal of Nuclear Science and Technology 34 (1997) 431

[8] C. Rubbia et al, CERN/AT-95-44-ET (1995)

[9] G. Duchéne, F. A. Beck, P. J. Twin, G. de France, D. Curien, L. Han, C. W. Beausang, M. A. Bentley, P. J. Nolan and J. Simpson, Nucl. Instr. and Meth. A 432 (1999) 90

[10] S. Dababneh, N. Patronis, P.A. Assimakopoulos, J. Görres, M. Heil, F. Käppeler, D. Karamanis, S. O'Brien and R. Reifart, submitted to Nucl. Instr. Meth. A

[11] C. L. Lee and X.-L. Zhou , Nucl. Instr. Meth. B 152 (1999) 1

[12] W. Ratynski and F. Käppeler, Physical Review C 37 (1988) 595

[13] GEANT4 Collaboration, CERN/LHCC 98-44

[14] N. Patronis, P. A. Assimakopoulos, D. Karamanis, S. Dababneh, M. Heil, F. Käppeler, R. Plag, P. E. Koehler, A. Mengoni and R. Gallino, in preparation

[15] A. A. Sonzogni, Nuclear Data Sheets 95 (2002) 837